photonics

MDPI

Article

He-Kr Gas-Discharge Laser Based on Hollow-Core Fiber

Igor Bufetov [1], Dmitry Komissarov [1], Sergey Nefedov [2], Alexey Kosolapov [1], Vladimir Velmiskin [1], Alexander Mineev [2] and Alexey Gladyshev [1,*]

[1] Prokhorov General Physics Institute of the Russian Academy of Sciences, Dianov Fiber Optics Research Center, 38 Vavilov St., 119991 Moscow, Russia; iabuf@fo.gpi.ru (I.B.); komdg@fo.gpi.ru (D.K.); kaf@fo.gpi.ru (A.K.); vvv@fo.gpi.ru (V.V.)

[2] Prokhorov General Physics Institute of the Russian Academy of Sciences, 38 Vavilov St., 119991 Moscow, Russia; nnssmm@yandex.ru (S.N.); mineev@kapella.gpi.ru (A.M.)

* Correspondence: alexglad@fo.gpi.ru

Abstract: Recently, two completely different types of lasers—a fiber laser and a gas-discharge laser—were combined into a single device by demonstrating 2.03 μm laser generation in He-Xe plasma that was produced by a microwave discharge directly inside a hollow-core fiber. This new type of laser—a gas-discharge fiber laser—provides excellent opportunities to greatly enrich the wavelength range of the operation of fiber lasers. In this work, we investigate a He-Kr gas mixture as an active medium of this new type of laser. As a result, a He-Kr gas-discharge fiber laser is demonstrated for the first time. The laser was pumped by a microwave discharge in a He:Kr (40:1) mixture that was filled into a revolver fiber with the hollow-core diameter of 130 μm. The total gas pressure was about 100 torr. With broadband mirrors of the laser resonator, generation was observed simultaneously at wavelengths of 2190 and 2523 nm. The output power of the He-Kr gas-discharge fiber laser was about 1 mW.

Keywords: hollow-core fiber; gas discharge; fiber laser; gas laser; microwave

Citation: Bufetov, I.; Komissarov, D.; Nefedov, S.; Kosolapov, A.; Velmiskin, V.; Mineev, A.; Gladyshev, A. He-Kr Gas-Discharge Laser Based on Hollow-Core Fiber. *Photonics* **2024**, *11*, 1102. https://doi.org/10.3390/photonics11121102

Received: 28 October 2024
Revised: 18 November 2024
Accepted: 20 November 2024
Published: 22 November 2024

1. Introduction

Gas-filled hollow-core fibers (HCFs) have enabled numerous opportunities in the field of gas-based photonics and fiber optics [1–4]. One of these opportunities is to merge gas-discharge lasers and fiber lasers into a single device—a gas-discharge fiber laser (GDFL).

The idea behind the GDFL is rather straightforward—an electrical discharge should be somehow ignited inside a gas-filled HCF, thus forming an active medium, and this active HCF should be placed between two mirrors, which form the laser cavity. Each component of such a laser would add its own advantages to the final device. First, the low-loss HCF would provide a very long interaction length, while still maintaining the compactness of a flexible fiber coiled on a spool. Second, a variety of active gas mixtures would enable access to an enormous number of wavelengths spanning from the ultraviolet to mid-infrared range, thus far surpassing solid-state fiber lasers, which are based on a limited number of active ions. Importantly, the hollow-core fibers do support low-loss transmission in the wide spectral range mentioned. Third, the electric discharge would provide a unified pumping scheme that does not rely on other lasers and does not require precise matching to the narrow absorption lines of the gases used. And forth, the spectral selectivity of the cavity mirrors would provide a choice of desired wavelengths.

Although steps towards gas-discharge fiber lasers have been undertaken since 2007 [5], the first GDFLs have been demonstrated only recently [6,7]. To realize the GDFL, the key was a suitable pumping scheme, which was based on the application of a microwave (2.45 GHz) electric field across the gas-filled HCF. This pumping scheme not only enables the contactless and stable maintenance of the discharge inside a hollow core of a small diameter (~130 μm), but also leaves both ends of the HCF free for coupling to the cavity mirrors.

The reported GDFLs relied on neutral Xe atoms, one of the transitions of which resulted in lasing at a wavelength of 2.03 μm [6,7]. The output characteristics of the laser were similar, when both three-component (He:Ar:Xe, 100:10:1) [6] and two-component (He:Xe, 100:1) [7] gas mixtures were used. An investigation into other gas mixtures is of evident interest, since it is one way to extend the wavelength range of the GDFL's operation.

In this work, a helium–krypton mixture as an active medium of the GDFL is investigated. As a result, the He-Kr gas-discharge fiber laser is demonstrated for the first time. The laser generates in a quasi-continuous wave regime with a total output power of about 1 mW. Based on the transitions of neutral krypton atoms, the lasing is observed simultaneously at the wavelengths of 2190 and 2523 nm.

2. Materials and Methods

The scheme of the gas-discharge fiber laser (Figure 1a) includes a 120 cm long piece of revolver-type HCF (1) with a hollow core diameter of 130 μm. A microphotograph of the fiber cross-section and transmission spectrum of the fiber are shown in Figures 1b and 2, respectively. The ends of the HCF were hermetically fixed in small vacuum chambers (2) that had a gas inlet/outlet to enable evacuation of the hollow core down to a pressure of ~10^{-2} torr and then filling it with a required gas mixture. In our experiments, the He:Kr mixtures were used as an active medium. The laser cavity was formed by plane mirrors, a highly reflective (HR) mirror and an output coupler (OC), both of which were attached to the vacuum chambers via sylphons that allowed fine alignment of the cavity.

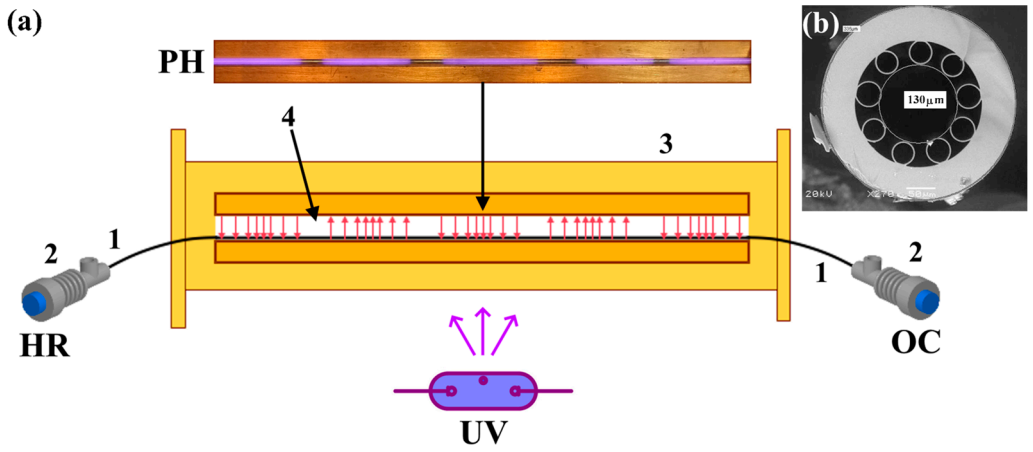

Figure 1. (**a**) The scheme of experimental setup. 1—Revolver-type hollow-core fiber; 2—small vacuum chambers; 3—a section of a microwave waveguide; 4—a slit in the side surface of the waveguide. Red arrows illustrate direction and intensity of the microwave electric field E_0 in the slit. HR—high-reflection mirror; OC—output coupler; UV—mercury lamp for the discharge ignition. The inset PH shows a real photograph of microwave discharge luminescence in the hollow-core fiber placed in the slit. (**b**) Microphotograph of the hollow-core fiber cross-section.

A 30 cm long middle section of the fiber was placed in a slit (4) that was made in the side wall of a special metallic microwave waveguide (3). The length and width of the slit were 32 cm and 2 mm, respectively. The waveguide had a rectangular cross-section of 90 × 45 mm and supported a single-mode propagation of H_{10} wave at the frequency of 2.45 GHz. One end of the waveguide was short-circuited by a metallic plunger.

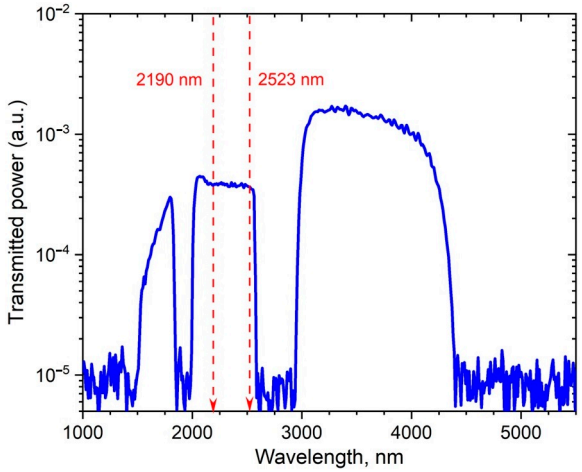

Figure 2. Transmission spectrum of the hollow-core fiber used in the experiments. Red dashed lines point out the wavelengths, at which lasing of the He-Kr GDFL is observed in this work.

To apply a microwave electric field across the HCF, the open end of the waveguide (3) was coupled to a magnetron (not shown) generating at a frequency of 2.45 GHz in pulsed mode. The pulse repetition rate was 400 Hz, while the pulse duration ranged from 20 to 80 μs. The peak power of microwave radiation in the waveguide was varied in the range from 1.4 to 3.2 kW. This microwave power defines unambiguously the average amplitude of a microwave electric field E_0 that is applied across the hollow-core fiber mounted in the slit (4). We determined the value of E_0 both by estimates on the basis of the simple analytical model we proposed earlier [8], and by numerical simulation of microwave pulse propagation in the waveguide we used. Both methods gave similar results, showing that in our experimental conditions, the value of E_0 was varied in the range from 3.6 to 5.3 kV/cm. Throughout the paper, it is the value of E_0 that will be used for the indication of the pump level for the GDFL.

Applying the microwave electric field across the HCF was not enough to initiate the discharge. That is why short-time (~1 s) irradiation by UV light of a mercury lamp was implemented to pre-ionize the gas mixture inside the hollow core. Since the fiber is coated by a polymer, which is highly absorptive for UV light, the polymer coating had to be removed from a ~1 cm long section of the HCF for the pre-ionization to work. After initiation, the discharge was stably maintained by a microwave electric field only, with the mercury lamp turned off.

The discharge took place in five fiber sections (Figure 1, inset PH), which correspond to the maxima of the standing wave pattern that is formed through interference of microwaves. Note, the uncoated section of the HCF was only present in one of the standing wave maxima, and thus, the discharge was initially ignited in that section only. Nevertheless, the discharge appears in all five sections with a delay of 1–2 μs relative to the leading edge of the microwave pulse. Such spreading of the discharge along the HCF becomes possible due to ability of the HCF to guide UV light. Ignited initially in the uncoated HCF section, the plasma emits UV radiation, some portion of which is guided along the hollow-core fiber and pre-ionizes the gas mixture in other sections of the fiber, thus initiating the discharge in those HCF sections that are located in the maxima of the microwave electric field.

It should be noted that the volume occupied by the discharge was as small as ~4 mm^3, which is much less compared with the ~10^6 mm^3 volume of that part of the gas filling system, which was permanently connected to the HCF. Therefore, the equilibrium pressure in the hollow core remained almost constant during the experiments.

The cavity mirrors, both HR and OC, were chosen to be as broadband as possible. The HR mirror was made of a mechanically polished aluminum plate, while a polished silicon plate with multilayer coating was used as an output mirror (OC). Spectra of the effective reflectivity for both mirrors in the wavelength range from 1.5 to 3.5 μm are

shown in Figure 3. The spectra were obtained on the basis of reflectivity of polished aluminum [9] and the measured transmission spectrum of the OC used [6]. The mirrors were pre-aligned to minimize the optical losses of the cavity before the beginning of laser experiments. The separation distance between the ends of the fiber and the cavity mirrors was about D ~ 100 μm, which is much less compared to Rayleigh range of the output beam Z_R ~ 3.5 mm and, thus, provides efficient back-coupling of laser radiation.

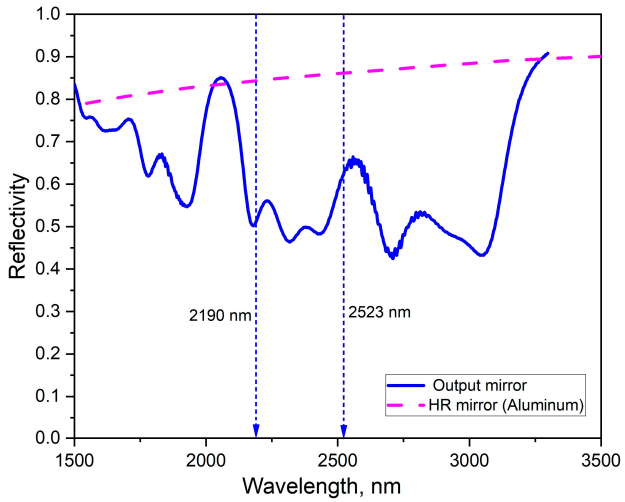

Figure 3. Reflection spectra of the mirrors that formed the cavity of He-Kr gas-discharge fiber laser. Blue dashed lines point out the wavelengths, at which lasing of the He-Kr GDFL was observed.

The radiation emitted through the cavity output mirror (OC) was registered by using (1) a photoresistor with high sensitivity in a spectral range from 1500 to 4500 nm complemented by a set of band-pass optical filters, (2) an optical spectrum analyzer with spectral range from 1200 to 2400 nm (AQ6375B, Yokogawa, Tokyo, Japan), and (3) a monochromator (MS2004, SOLAR TII, Minsk, Belarus) for the range from 1600 to 3700 nm followed by the photoresistor mentioned above. The time resolution of the photoresistor was about ~3 μs.

The radiation of the discharge plasma emitted through the side surface of the HCF was collected by multimode silica fiber and registered by silicon photodetector with a time resolution of at least 0.1 μs. Spectral composition of this radiation was also measured in the range from 200 to 1100 nm by using a spectrometer (Flame-TXPI-ES, Ocean Insight, Dunedin, FL, USA). A detailed description of the experimental setup and justification of the chosen discharge excitation scheme in the HCF can be found in [6–8].

3. Results and Discussion

He:Kr gas mixtures with different mole fractions of krypton were studied as an active medium of the GDFL. The use of pure krypton can provide a longer operating time of the gas laser due to the absence of cataphoresis [10]. At the same time, it is known that the addition of helium as a buffer gas provides higher optical gain for the discharges in noble gases. Moreover, the laser generation in the noble gas mixtures with helium is observed at a greater number of wavelengths [11–13].

In our experiments with pure krypton at a pressure of about 100 torr, the microwave discharge in the HCF was easily excited and maintained, but laser generation was not observed. When helium was added into the gas mixture, the lasing was detected only at a sufficiently low krypton content, namely, at 2.5 and 1% (Figure 4). Although the microwave discharge was maintained at higher mole fractions of krypton, laser generation was not observed. In the opposite case, when the Kr mole fraction was below 1%, the discharge itself was not maintained, even if the maximum electric field value of E_0 = 5.3 kV/cm was applied across the HCF (Figure 4).

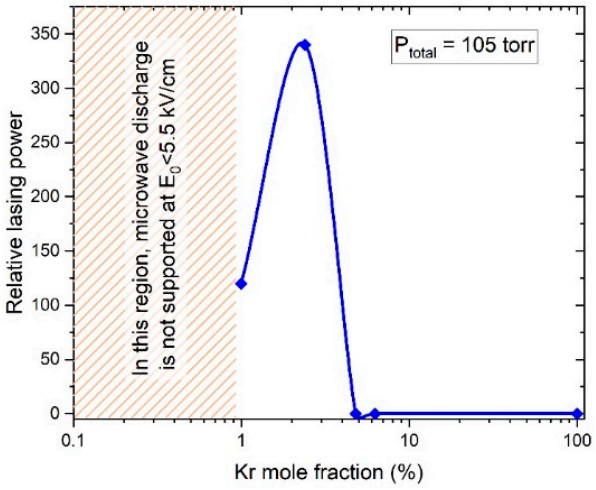

Figure 4. Relative peak output power of the He-Kr GDFL as a function of mole fraction of Kr atoms. Total pressure of the He-Kr gas mixture was 105 torr.

The He:Kr mixture with Kr mole fraction of 2.5% was chosen for further experiments. The mixture at a total pressure of 105 torr was filled into the HCF, which was kept inside a properly aligned laser cavity. Then, the microwave discharge was ignited and maintained, and the optical radiation at the cavity output mirror was investigated. Importantly, the optical signal was strongly dependent on the angular positions of the cavity mirrors, in a similar way to what was previously observed for a He:Xe GDFL [7]. In the case of the complete misalignment of the cavity, the optical signal dropped by several order of magnitude, thus directly indicating the laser nature of the recorded signal. Also, the stability of the He:Kr GDFL appeared to be similar to that of the He:Xe GDFL [14].

Figure 5 illustrates typical waveforms registered by the photoresistor at the output of the He-Kr GDFL for two values of the microwave pump pulse duration: 20 μs (Figure 5a) and 80 μs (Figure 5b). In contrast to the He-Xe GDFL [6,7], in which the pump power practically did not affect the shape and power of the output pulses, the pulses generated by the He-Kr laser show a pronounced dependance on the pump power. As can be seen in Figure 5, the amplitude of the laser pulses is growing with a decrease in the amplitude of a microwave electric field E_0 that is applied across the hollow-core fiber. At high pumping levels ($E_0 > 5.5$ kV/cm), laser generation was completely absent. However, when the pump was decreased to $E_0 \approx 5.4$ kV/cm, the first indications of lasing appear after the trailing edge of the pump pulse, i.e., during the recombination of the discharge plasma (Figure 5a, curve 5). At the same time, the plasma glow that was registered from the side surface of the fiber (Figure 5a, curve 1) stops simultaneously with the end of the pump pulse (Figure 5a, curve 2). It should be noted that similar generation peaks, occurring after switching off the exciting pulse, were previously observed in bulk gas-discharge He-Ne lasers at different wavelengths [15]. In the case of He-Ne plasma, this phenomenon can be explained by the resonant transfer of energy from excited He atoms to Ne atoms. However, for the He-Kr gas mixture, such resonant transfer is not the case. Perhaps, to explain this phenomenon in He-Kr, one can use the mechanism of collisional mixing between the 4d-sublevels of excited Kr atoms [16] or the generation mechanisms of plasma lasers [17].

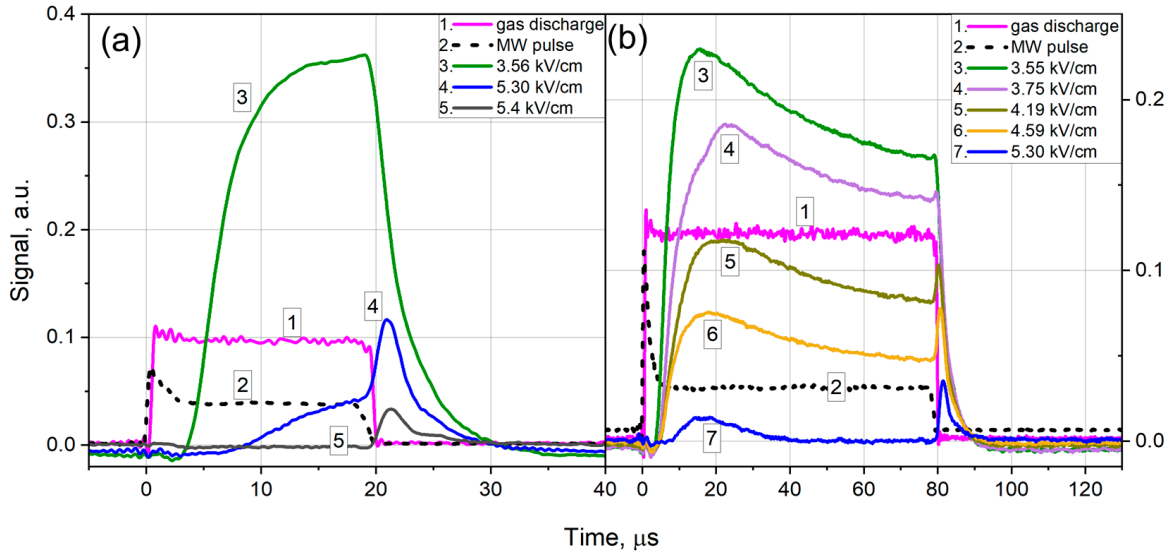

Figure 5. Typical waveforms measured by a photoresistor at the output of He-Kr GDFL for different values of a microwave electric field E_0 that is applied across the hollow-core fiber. The E_0 amplitudes are shown in the figure legend. The microwave pump pulse (curves 2) and the waveform of plasma discharge registered from the side surface of the fiber (curves 1) are also shown. The duration of pump pulses was (**a**) 20 μs and (**b**) 80 μs. Total pressure of the He-Kr mixture was 105 torr with Kr mole fraction of 2.5%.

Decreasing the microwave excitation to $E_0 < 5.3$ kV/cm gives rise to laser generation during the pump pulse (Figure 5). Note that the laser generation develops with a delay of about 5 μs relative to the leading edge of the pump pulse. The output power of the He-Kr GDFL increases monotonously until the microwave electric field reaches a value of $E_0 \approx 3.6$ kV/cm, at which point, the discharge itself becomes unstable and quenches. A similar dependence is known for bulk gas-discharge lasers (see, e.g., [18]), in which the output power initially grows with the pump, but then reaches a maximal value and starts falling with further pump increase. In our case, however, due to the limited range of E_0 variation available in our setup, we probably observe only the falling branch of the $P_{out}(E_0)$ dependence.

The peak power generated by He-Kr GDFL was investigated as a function of the total gas pressure (Figure 6). When the pressure was above ~130 torr, laser generation did not occur, although the discharge was maintained stably. With the pressure gradually decreasing below 130 torr, the generation power first increases and passes through a maximum, which is observed at different pressures for different values of the microwave field E_0. Then, the output power is slightly reduced before the discharge itself is no longer maintained at pressures below ~70 torr.

The variations in the shape of the laser pulses observed in Figure 5 may indicate that we are dealing with generation at several wavelengths and with competition between these generation channels. By passing the GDFL radiation through band-pass optical filters, we found that the laser spectrum contains some lines in the wavelength ranges of 1750–2250 nm and 2500–3000 nm. Then, the emission spectra of He-Kr GDFL were studied in more detail by using an optical spectrum analyzer (AQ6375B, Yokogawa, Tokyo, Japan) with a spectral range of 1200–2400 nm (Figure 7a,b) and a grating-based monochromator (MS2004, SOLAR TII, Minsk, Belarus) with spectral range of 1600–3700 nm (Figure 7c). The spectrum analyzer and the monochromator had resolutions of 0.1 and 2 nm, respectively, which is good enough to identify the lasing lines of gas lasers [19].

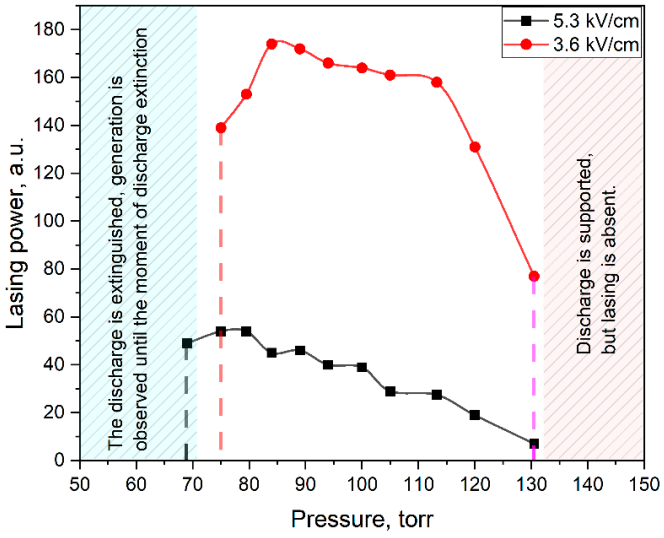

Figure 6. Peak power generated by He-Kr GDFL as a function of total gas pressure. The mole fraction of Kr was 2.5%. The amplitude of the microwave field E_0 was 3.6 kV/cm (red dots) and 5.3 kV/cm (black squares).

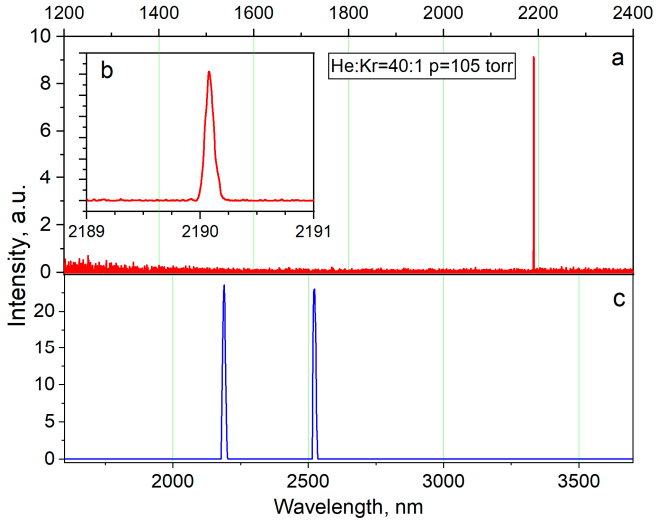

Figure 7. Typical output spectra generated by He-Kr GDFL based on He-Kr mixture at a total pressure of 105 torr and Kr mole fraction of 2.5%. The spectra were measured (**a**,**b**) by optical spectrum analyzer AQ6375B (Yokogawa) in 1200–2400 nm range and (**c**) by grating-based monochromator MS2004 (SOLAR TII) in 1600–3700 nm range.

The spectra obtained show that, in our experimental conditions, the He-Kr GDFL generates simultaneously at two wavelengths, which are 2190 and 2523 nm (Figure 7). The observed linewidth for both lasing lines did not exceed the spectral resolution of the devices used for the measurement. Based on the spectra obtained and the spectral sensitivity of the photoresistor used, the total output peak power of the He-Kr GDFL was found to be around 1 mW. One should keep in mind that this power is obtained from a tiny volume of active medium, which was as small as 4 mm^3. The output power of the laser can be increased by using a much longer length of the active fiber that is pumped by the microwave electric field. Also, the GDFL performance could be improved by optimizing the active medium composition and the laser cavity structure.

The shapes of the laser pulses at wavelengths of 2190 and 2523 nm differ from each other (Figure 8). Generation at 2523 nm occurs with a longer delay relative to the leading edge of the microwave pump pulse and increases more slowly in time compared with generation at 2190 nm. While the power generated at 2190 nm reaches a maximum and

then decreases (Figure 8a,b, curves 1), we did not observe such a power decrease at the wavelength of 2523 nm (Figure 8a,b, curves 2). The difference in the shapes of the laser pulses observed at different wavelengths is probably due to differences in the parameters of the upper laser levels, which determine the rates of their population and relaxation during microwave discharge.

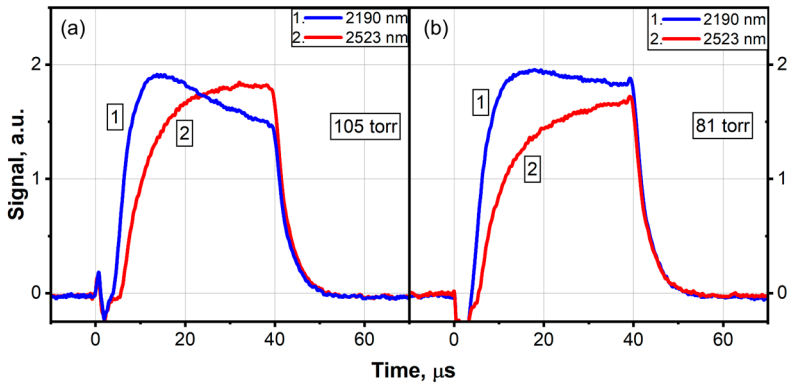

Figure 8. Typical waveforms generated by He-Kr GDFL and measured separately for the line at 2190 nm (curves 1) and the line at 2523 nm (curves 2). The data were obtained in the He-Kr mixture with a 2.5% mole fraction of Kr and at total pressure of (**a**) 105 torr and (**b**) 81 torr.

The laser lines generated by the He-Kr GDFL correspond to transitions in a neutral krypton atom (Kr I). Those transitions are well known from the data on bulk (non-fiber) gas-discharge lasers obtained earlier (see, for example, ref. [19]). The laser line at 2190 nm occurs on the $4d[3/2]_2^0 \rightarrow 5p[3/2]_2$ transition, while the $4d[1/2]_1^0 \rightarrow 5p[3/2]_2$ transition gives rise to generation at 2523 nm. These transitions have different upper energy levels, but a common lower level, which can lead to the competition of lasing processes when both transitions are involved simultaneously (see the diagram in Figure 9). Please note that the common lower level $5p[3/2]_2$ mentioned above is also the upper level for the transition $5p[3/2]_2 \rightarrow 5s[3/2]_2^0$ at a wavelength of 760.2 nm, luminescence at which we can observe in the discharge spectrum measured from the side surface of the fiber. Thus, the 760.2 nm luminescence line of Kr atoms can serve as an indicator for the population of the lower laser level.

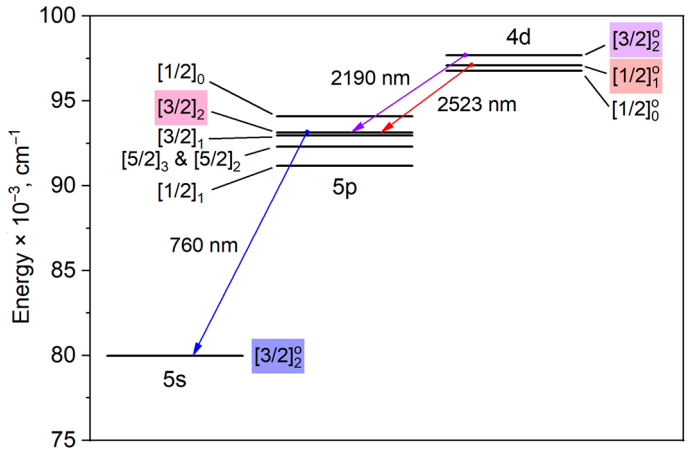

Figure 9. The scheme of krypton energy levels involved in the He-Kr laser generation. A transition responsible for luminescence at 760 nm is also shown, since it serves as an indicator of population of lower laser level for both laser transitions observed in this work.

To obtain some insight into the influence of He on the population of Kr energy levels, we monitored the discharge luminescence spectra from the side surface of the HCF for

different concentrations of He. The luminescence spectra measured for strong microwave excitation (E_0 < 5.3 kV/cm) are shown in Figure 10. One can see that when helium is introduced as a buffer gas into the core of the HCF, the luminescence spectrum is enriched by emission lines of neutral helium atoms (He I), in particular at 502, 588, 668, and 707 nm (Figure 10, lines 1–4). The intensity of the He I lines increases with the helium concentration. At the same time, the intensity of the Kr I luminescence at 760 nm (Figure 10, line 5) is decreasing relative to other luminescence lines of Kr I, most evidently to the line at 810 nm (Figure 10, line 6) that is not connected with lasing transitions observed in the He-Kr GDFL. Thus, we conclude that the addition of helium to krypton has a significant effect on the population of the lower laser level $5p[3/2]_2$. Helium as a buffer gas reduces the population of the lower laser level and provides better conditions for laser generation.

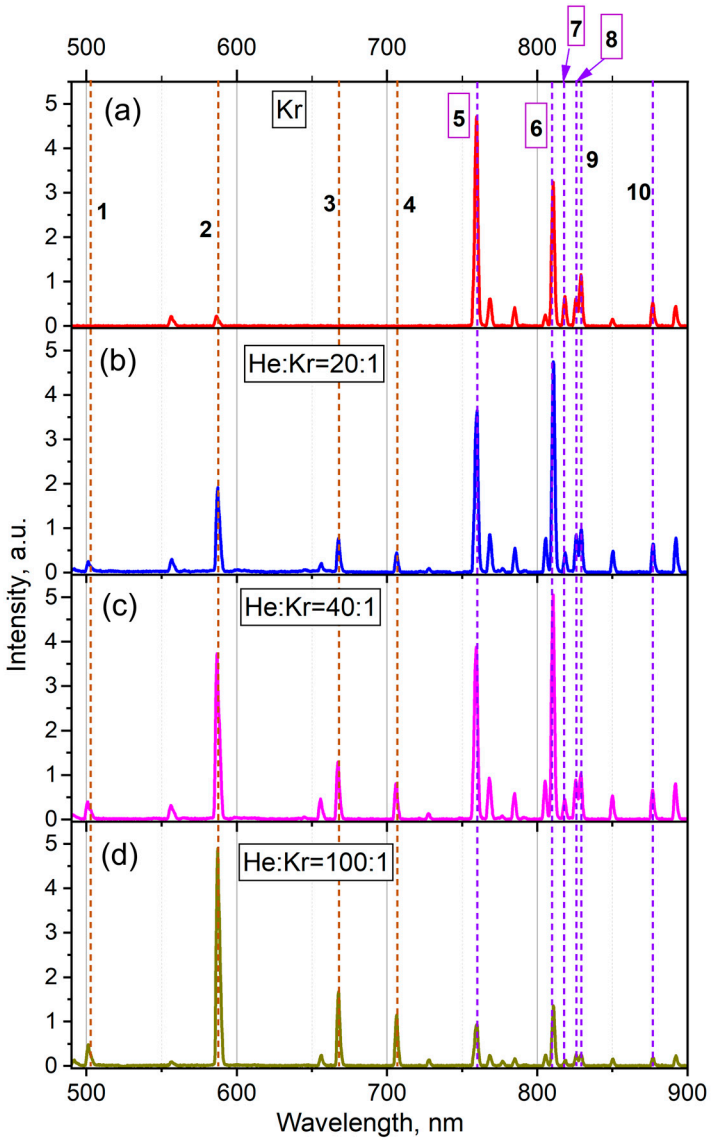

Figure 10. Plasma luminescence spectra measured from the side surface of the fiber for different concentrations of He in the He-Kr mixture. The amplitude of the microwave excitation was E_0 = 5.3 kV/cm. The following gas mixtures were studied: (**a**) pure Kr at pressure of 30 torr, (**b**) He:Kr = 20:1 at total pressure of 105 torr, (**c**) He:Kr = 40:1 at total pressure of 105 torr, (**d**) He:Kr = 100:1 at total pressure of 105 torr. The wavelengths of lines (1–10) and their relation to He or Kr are explained in Figure 11.

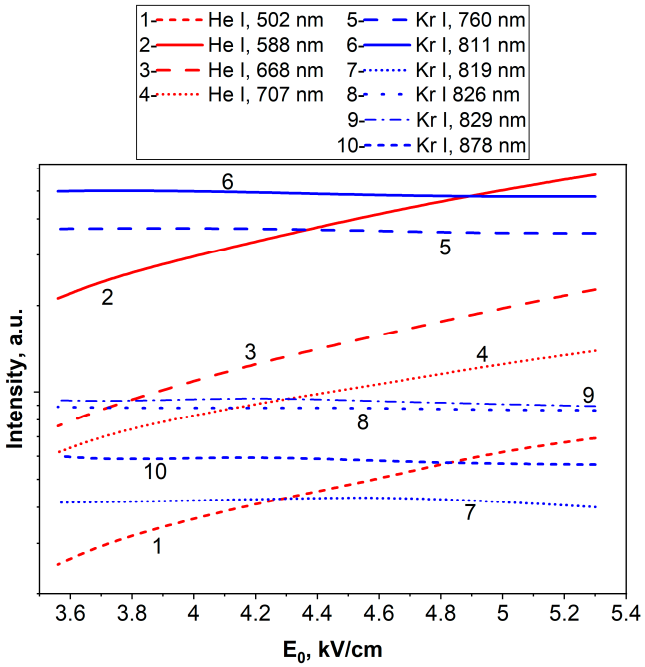

Figure 11. Intensities of He I and Kr I luminescence lines as a function of the microwave pump field E_0 applied across the hollow-core fiber. The measurements were performed with a He-Kr mixture at a total pressure of 105 torr and Kr mole fraction of 2.5%.

The influence of a lasing process on Kr I luminescence lines can be estimated by the data presented in Figure 11, where the intensities of the He I and Kr I luminescence lines are shown as a function of the microwave pump field E_0 applied across the hollow-core fiber. When the microwave field E_0 changes from 3.6 to 5.3 kV/cm, the lasing goes from its maximum to a complete termination. Figure 11 shows that the variation in the pump field affects the luminescence intensity of the main He I lines in the visible and near-IR ranges. When the pump changes in the considered range, the intensity of the He I lines increases proportionally $(E_0)^{2–2.5}$, while the intensity of the Kr I lines, on the contrary, decreases, but much more slowly (Figure 11). At the same time, the ratio of the amplitudes for the 760 nm (Kr I) and 810 nm (Kr I) lines shows almost no changes. This fact suggests that the presence of laser generation in the discharge plasma does not significantly affect the population of the lower laser level $5p[3/2]_2$. As for the upper laser levels ($4d[3/2]_2^0$ and $4d[1/2]_1^0$), the luminescence spectra provide no information due to the lack of convenient luminescence lines in the visible range starting from these levels [20].

4. Conclusions

A He-Kr gas-discharge fiber laser is demonstrated for the first time. The laser generates in a quasi-continuous wave regime simultaneously at the wavelengths of 2190 and 2523 nm, which corresponds to transitions in the neutral Kr atoms. The maximum output power of the He-Kr GDFL was about 1 mW and was obtained from an active volume as small as 4 mm^3 (a 30 cm long hollow core with a diameter of 130 μm). The operation conditions, such as the pressure of the gas mixture, the Kr molar fraction, and the microwave pump field, were determined.

The results obtained illustrate that the concept of gas-discharge fiber lasers can be applied in various gas media. GDFLs provide excellent opportunities to greatly enrich the wavelength range of the operation of fiber lasers, since a variety of active gas mixtures could enable access to an enormous number of wavelengths spanning from the ultraviolet to mid-infrared range. At the same time, the electric discharge could provide a unified pumping scheme that does not rely on other lasers and does not require precise matching to narrow absorption lines of the gases used. We believe that in the future, the GDFLs

could be used not only as a scientific instrument, but also could find various applications in spectroscopy, environmental monitoring and medical diagnostics.

Author Contributions: Conceptualization, I.B. and A.G.; methodology, A.M., S.N., I.B., D.K. and A.G.; formal analysis, I.B.; investigation, S.N., A.G., D.K., I.B. and A.M.; resources, A.K. and V.V.; writing—original draft preparation, I.B.; writing—review and editing, A.G., A.M. and I.B.; visualization, A.G.; supervision, A.G., I.B. and A.M.; project administration, A.G.; funding acquisition, A.G. and I.B. All authors have read and agreed to the published version of the manuscript.

Funding: This research was supported by the Russian Science Foundation (grant No. 22-19-00542), https://rscf.ru/en/project/22-19-00542/ (accessed on 27 October 2024).

Institutional Review Board Statement: Not applicable.

Informed Consent Statement: Not applicable.

Data Availability Statement: The data that support the findings of this study are available from the corresponding author, A.G., upon reasonable request.

Conflicts of Interest: The authors declare no conflicts of interest.

References

1. Russell, P.S.J.; Hölzer, P.; Chang, W.; Abdolvand, A.; Travers, J.C. Hollow-core photonic crystal fibres for gas-based nonlinear optics. *Nat. Photon.* **2014**, *8*, 278–286. [CrossRef]
2. Debord, B.; Amrani, F.; Vincetti, L.; Gérôme, F.; Benabid, F. Hollow-Core Fiber Technology: The Rising of "Gas Photonics". *Fibers* **2019**, *7*, 16. [CrossRef]
3. Fokoua, E.N.; Mousavi, S.A.; Jasion, G.T.; Richardson, D.J.; Poletti, F. Loss in hollow-core optical fibers: Mechanisms, scaling rules, and limits. *Adv. Opt. Photon.* **2023**, *15*, 1–85. [CrossRef]
4. Pryamikov, A.D.; Gladyshev, A.V.; Kosolapov, A.F.; Bufetov, I.A. Hollow-core optical fibers: Current state and development prospects. *Phys. Usp.* **2024**, *67*, 129–156. [CrossRef]
5. Shi, X.; Wang, X.B.; Jin, W.; Demokan, M.S.; Zhang, X.L. Progress toward a novel hollow-core fiber gas laser. In Proceedings of the SPIE 6767 Photonic Crystals and Photonic Crystal Fibers for Sensing Applications III, 67670H, Boston, MA, USA, 8 October 2007. [CrossRef]
6. Gladyshev, A.V.; Komissarov, D.G.; Nefedov, S.M.; Kosolapov, A.F.; Velmiskin, V.V.; Mineev, A.P.; Bufetov, I.A. Gas-Discharge Fiber Laser with Microwave Pumping. *Bull. Lebedev Phys. Inst.* **2023**, *50*, 403–408. [CrossRef]
7. Gladyshev, A.W.; Komissarov, D.G.; Nefedov, S.M.; Kosolapov, A.F.; Velmiskin, V.V.; Mineev, A.P.; Bufetov, I.A. Gas-Discharge He-Xe Fiber Laser. *IEEE J. Sel. Top. Quantum Electron.* **2024**, *30*, 0900107. [CrossRef]
8. Gladyshev, A.; Nefedov, S.; Kolyadin, A.; Kosolapov, A.; Velmiskin, V.; Mineev, A.; Bufetov, I. Microwave Discharge in Hollow Optical Fibers as a Pump for Gas Fiber Lasers. *Photonics* **2022**, *9*, 752. [CrossRef]
9. Smith, D.Y.; Shiles, E.; Inokuti, M. The Optical Properties of Metallic Aluminum. In *Handbook of Optical Constants of Solids*; Academic Press: New York, NY, USA, 1985; pp. 369–406.
10. Clark, P.O. Investigation of the Operating Characteristics of the 3.5 μm Xenon Laser. *IEEE J. Quantum Electron.* **1965**, *1*, 109. [CrossRef]
11. Paananen, R.A.; Bobroff, D.L. Very high gain gaseous (Xe-He) optical maser at 3.5 μ. *Appl. Phys. Lett.* **1963**, *2*, 99–100. [CrossRef]
12. Aisenberg, S. The effect of helium on electron temperature and electron density in rare gas lasers. *Appl. Phys. Lett.* **1963**, *2*, 187–189. [CrossRef]
13. Grant, K.J. Optimisation of neutral rare gas laser continuous wave power in the mid infra-red. *Infrared Phys. Technol.* **1995**, *36*, 1131–1133. [CrossRef]
14. Gladyshev, A.; Komissarov, D.; Nefedov, S.; Kosolapov, A.; Velmiskin, V.; Mineev, A.; Bufetov, I. Towards Mid-Infrared Gas-Discharge Fiber Lasers. *Photonics* **2024**, *11*, 242. [CrossRef]
15. Petrash, G.G.; Knyazev, I.N. Study of pulsed laser generation in Neon and in mixtures of Neon and Helium. *Sov. Phys. JETF* **1964**, *18*, 571–575. Available online: http://jetp.ras.ru/cgi-bin/dn/e_018_03_0571.pdf (accessed on 28 October 2024).
16. Verkhoglyad, A.G.; Krivoshchekov, G.V.; Kurbatov, P.F. Nature of Xe I laser line superradiance in the presence of a buffer gas. *Sov. J. Quantum Electron.* **1984**, *14*, 201–205. [CrossRef]
17. Gudzenko, L.I.; Shelepin, L.A.; Yakovlenko, S.I. The theory of plasma lasers. In *Theoretical Problems in Spectroscopy and Gas Dynamics of Lasers*; Basov, N.G., Ed.; Springer Science: New York, NY, USA; Business Media: New York, NY, USA, 1977; pp. 103–149. [CrossRef]
18. Sakurai, T. Dependence of He-Ne laser output on discharge current, gas pressure and tube radius. *Jpn. J. Appl. Phys.* **1972**, *11*, 1826–1831. Available online: https://iopscience.iop.org/article/10.1143/JJAP.11.1826/meta (accessed on 15 October 2024). [CrossRef]

19. Weber, M.J. *Handbook of Lasers*; CRC PRESS: Boca Raton, FL, USA, 2001.
20. Kramida, A.; Ralchenko, Y.; Reader, J.; NIST ASD Team. *NIST Atomic Spectra Database (Version 5.11)*; National Institute of Standards and Technology: Gaithersburg, MD, USA, 2023. Available online: https://physics.nist.gov/asd (accessed on 15 October 2024). [CrossRef]